【Natural Resource Letter】

Screening for inhibitory effects of crude drugs on furin-like enzymatic activities

Yuka Kiba[1], Rio Oyama[2], Sae Misawa[2], Takashi Tanikawa[3], Masashi Kitamura[1*], Ryuichiro Suzuki[2*]

[1] Laboratory of Pharmacognocy, School of Pharmacy, Faculty of Pharmacy and Pharmaceutical Sciences, Josai University; 1–1, Keyakidai, Sakado, Saitama 350–0295, Japan

[2] Laboratory of Natural Products & Phytochemistry, Department of Pharmaceutical Sciences, Faculty of Pharmacy and Pharmaceutical Sciences, Josai University, 1–1, Keyakidai, Sakado, Saitama 350–0295, Japan

[3] Laboratory of Nutri-pharmacotherapeutics Management, School of Pharmacy, Faculty of Pharmacy and Pharmaceutical Sciences, Josai University; 1–1, Keyakidai, Sakado, Saitama 350–0295, Japan

*Corresponding author

Tel and Fax: +81 49 271 8021

E-mail: kitamura@josai.ac.jp

ryu_suzu@josai.ac.jp

Abstract

The spike (S) protein of severe acute respiratory syndrome coronavirus 2 (SARS-CoV-2) contains a cleavage motif R-X-X-R for furin-like enzymes at the boundary of the S1/S2 subunits. The cleavage of the site by cellular proteases is essential for S protein activation and virus entry. We screened the inhibitory effects of crude drugs on *in vitro* furin-like enzymatic activities using a fluorogenic substrate with whole-cell lysates. Of the 124 crude drugs listed in the Japanese Pharmacopeia, aqueous ethanolic extract of Cnidii Monnieris Fructus, which is the dried fruit of *Cnidium monnieri* Cussion, significantly inhibited the furin-like enzymatic activities. We further fractionated the plant extract and isolated the two active compounds with the inhibitory activity, namely, imperatorin and osthole, whose IC_{50} values were 1.45 mM and 9.45 μM, respectively. Our results indicated that Cnidii Monnieris Fructus might exert inhibitory effects on furin-like enzymatic activities, and that imperatorin and osthole of the crude drug could be potential inhibitors of the motif cleavage.

Keywords: furin, proprotein convertase, SARS-CoV-2, coumarin, imperatorin, osthole

Introduction

In December 2019, a novel virus, severe acute respiratory syndrome coronavirus 2 (SARS-CoV-2), belonging to the human coronavirus family, was identified in Hubei Province, China [1]. It causes coronavirus disease 2019 (COVID-19), a severe respiratory disease associated with a high mortality rate. According to the World Health Organization 2019 situation report of February 16, 2021, more than 100,000,000 patients have been diagnosed with COVID-19 and 2,300,000 have died worldwide. The entry of coronavirus into host cells is mediated by the spike (S) protein [2]. Processing of the S protein by cellular proteases such as transmembrane protease serine 2 (TMPRSS2), cathepsin, and furin is necessary for protein activation and virus entry [3]. The S protein of SARS-CoV-2 consists of the N-terminal S1 domain and C-terminal S2 domain [2, 3]. The S1 domain has a receptor-binding domain (RBD) that binds to the host angiotensin-converting enzyme 2 (ACE2) receptor and the S2 domain has an fusion peptide (FP) domain that mediates membrane fusion. The S protein cleavage at the S1/S2 boundary by host cell protease plays a key role in binding the ACE2 receptor to the S1 domain. The S protein of SARS-CoV2 has a cleavage motif R-X-X-R for furin-like enzymes at the S1/S2 boundary, matching the consensus amino acid motif of the substrate for furin and related proprotein convertases (PCs) [2, 3]. Furin/PC inhibitors block SARS-CoV-2 S protein cleavage to suppress viral entry [2-5]. In addition, SARS-CoV-2 pseudoviruses, which have a mutated S protein at the cleavage site, showed substantially decreased efficiency of entry into host cells [2-4]. Therefore, cleavage inhibitors of the motif site are expected to be therapeutic reagents for SARS-CoV-2 infection [6-8].

Furin, a member of the proprotein convertase family, is ubiquitously expressed in mammalian cells and activates various proprotein substrates [9-11]. Furin regulates not only pathogenic pathways but also several physiological pathways, involving hormones, growth factors, adhesion molecules, and cell surface receptors [12]. Furin is involved in calcium-dependent proteolytic cleavage at the C-terminus of a consensus amino acid motif R-X-X-R↓ (the arrow indicates the cleavage position) [9].

Peptide-based small molecules such as hexa-D-arginine (D-6R) and chloromethylketone (CMK) have been reported to be inhibitors of furin and other PCs [13-18]. However, furin/PC-targeting therapeutic reagents for clinical application have not been identified to date. Numerous studies have evaluated furin-like (furin and other PCs) enzymatic activities using a fluorogenic substrate with whole cell lysates and tissue homogenates [19-24]. In this study, the inhibitory effects of crude drugs were evaluated using the furin-like protease assay with a fluorescent peptide substrate.

Materials and methods

Materials

We selected 124 crude drugs listed in the Japanese Pharmacopeia, 17th Edition, and purchased them from several distributors (Supplementary Material, Table S1) [25]. Crude drugs (10 g) were refluxed with 300 ml of 70% EtOH for 1 h, and the resultant extracts were dried by evaporation. The samples were dissolved in dimethyl sulfoxide (DMSO) to a concentration of 10 mg/ml and stored at 4°C until use. Imperatorin and osthole were obtained from Tokyo Chemical Industry Co., Ltd. (Tokyo, Japan) and FUJIFILM Wako Pure Chemical Corporation (Osaka, Japan), respectively.

Furin-like enzyme assay

A549 cells, human lung carcinoma epithelial cells, were obtained from RIKEN BioResource Center (Tsukuba, Japan) and cultured in Dulbecco's modified Eagle's medium containing 10% fetal bovine serum, 100 µg/ml streptomycin, and 100 units/ml penicillin. A549 cells were seeded in 100-mm-diameter dishes (1.0×10^6 cells/plate) and cultured for 24 h at 37°C with 5% CO_2. After 24 h, the cells were washed twice with Dulbecco's phosphate-buffered saline (D-PBS). The washed cells were collected in a 1.5-ml tube by scraping and centrifuging at 2000 × *g* for 2 min. The cells were counted and treated with 1 ml of 2× lysis buffer (20 mM HEPES-KOH [pH 7.4], 0.5% Triton X-100, 1 mM $CaCl_2$) per 1.0×10^6 cells. The cell lysates were vortexed for 5 min and centrifuged at 13,000 × *g* for 10 min at 4°C. The supernatants were transferred to 1.5-ml tubes and stored at -80°C until use. Supernatants (10 µl), crude drug extracts (10 µl), and H_2O (70 µl) were added to a 96-well black microplate and incubated at 37°C for 30 min. Drug extracts were diluted and adjusted to a final concentration of 20 µg/mL for screening. To the mixture, 10 µl of 1 mM Pyr-Arg-Thr-Lys-Arg-methyl-coumaryl-7-amide (pyr-RTKR-MCA) was added (PEPTIDE INSTITUTE, Inc., Osaka, Japan). The mixture was incubated at 37°C for 30 min, and fluorescence intensity of the sample was measured with excitation at 380 nm and emission at 460 nm using SpectraMax M2 (Molecular Devices, LLC, CA, USA). The 124 samples were subjected to screening using the furin-like enzyme assay, and the results are presented as mean ± standard deviation of at least three independent experiments. Ethylenediaminetetraacetic acid (EDTA, final conc. 50 mM) was used as

the control in the assay. Half-maximal inhibitory concentration (IC_{50}) was obtained by logistic regression analysis using the *drc* package for R [26]

Extraction and isolation of the bioactive compounds

The dried fruits of *Cnidii monnieri* (100 g) were extracted three times with 70% aqueous EtOH (1 h, each) under reflux, and the solvent was evaporated in vacuo to obtain the corresponding extract (55 g). The extract was suspended in water and fractionated with ethyl acetate three times to obtain an ethyl acetate layer. The water-soluble portion was partitioned with *n*-BuOH three times. The yield of ethyl acetate soluble extract and *n*-BuOH soluble extract were 4.7 and 1.2 g, respectively. The ethyl acetate soluble extract (0.3 g) was subjected to chromatography on an ODS column (ODS-SM 50C; Yamazen Corporation, Osaka, Japan) with MeOH–H_2O (4:1, v/v) as a solvent to yield 16 fractions. Fraction 4 (12 mg) was chromatographed on a preparative HPLC column (Senshu Pak ODS-4151-N; 10 mm × 150 mm) eluted with MeOH–H_2O (2:1, v/v) and monitored at 254 nm to obtain **1** (5.2 mg). Fraction 6 (15 mg) was purified by HPLC (Senshu Pak ODS-4151-N; 10 mm × 150 mm) with MeOH–H_2O (2.8:1, v/v) as a solvent, and monitored at 254 nm to obtain **2** (12 mg).

Identification

Compounds **1** and **2** were identified as imperatorin and osthole, respectively. Their structures were confirmed by comparing their spectroscopic data, such as NMR and MS, with those of authentic compounds.

Results and Discussion

We screened 124 crude drug extracts for inhibitory effects on furin-like activities. The furin-like activity was evaluated using pyr-RTKR-MCA as a fluorogenic substrate and cell lysates as whole proteolytic enzyme. Of the 124 crude drug extracts, three extracts, Cnidii Monnieris Fructus (dried fruits of *C. monnieri*), Hydrangeae Dulcis Folium [dried leaves of *Hydrangea macrophylla* (Thunb.) Ser. var. *thunbergii* (Siebold) Makino)], and Forsythiae Fructus [dried fruit of *Forsythia suspensa* (Thunb.) Vahl] suppressed furin-like activities by more than 40% (activity: 6.2% ± 0.3%, 56.5% ± 1.8%, and 42.9% ± 2.3 %, respectively) (Table 1). We then evaluated the IC_{50} of the three samples and Cnidii Rhizome (the dried rhizome of *C. officinale*) as the control. The IC_{50} values of Cnidii Monnieris Fructus, Hydrangeae Dulcis Folium, and Forsythiae Fructus were 1.10, 7.12, and 6.52 μg/ml, respectively. Cnidii Monnieris Fructus showed stronger inhibitory effects on furin-like activity than Cnidii rhizome (IC_{50} > 50 μg/ml). Cnidii Monnieri Fructus (*Jashoshi* in Japanese) has been traditionally used to treat osteoporosis, sexual dysfunction, asthma, and skin ailments [27]. *Cnidium monnieri* Cusson contains several compounds such as bergapten, imperatorin, osthole, and xanthotoxin [28]. Here, we fractionated and isolated bioactive compounds from Cnidii Monnieris Fructus contributing to the inhibitory effects on furin-like enzymatic activity. We isolated and identified two coumarin compounds, imperatorin and osthole, with inhibitory activity (Fig.1). Osthole (IC_{50} = 9.45 μM) showed significant inhibitory effects on furin-like enzymatic activity compared with imperatorin (IC_{50} = 1.45 mM). The autofluorescence of two coumarins (imperatorin and osthole) did not occur because reaction mixture (compounds and substrates) without cell lysates did not show

fluorescence signal. These results indicate that Cnidii Monnieris Fructus might inhibit furin-like enzymatic activities, and that imperatorin and osthole of the crude drug could be candidates for inhibitors of motif cleavage.

In the present study, we screened the anti-furin-like activity of crude drugs using an *in vitro* furin-like assay with a fluorogenic substrate. Since furin is a Ca^{+}–dependent serine protease, EDTA, a popular chelating agent was used as positive control in this screening. However, a high concentration (IC_{50} 50 mM) was required to exert its inhibitory activities. Although polyphenols such as tannin is known to show chelating activities, our medicinal plant extracts containing polyphenols did not show inhibitory effects on furin-like activities. It is considered that the concentration of polyphenols in our medicinal extracts was not sufficient to exhibit inhibitory activity. Of the 124 crude drugs, *Cnidii* Monnieris Fructus showed strong inhibitory effects on furin-like activity, and two coumarin compounds (imperatorin and osthole) exerted inhibitory activity. Further studies are required to understand if Cnidii Monnieris Fructus and its bioactive compounds block S protein processing. For example, the inhibitory effect on S protein processing could be proven if the S protein expressed in *Escherichia coli* is used as a cleavage substrate instead of pyr-RTKR-MCA [29]. When the S protein gene was transfected into mammalian cells, the S protein was processed by furin/PC, and syncytial phenotype was observed [5, 30]. Evaluation of S protein processing by western blotting and syncytial formation by microscopy would provide direct evidence that the samples affect S protein processing and virus entry.

Osthole is a multifunctional compound with anti-oxidative, anti-proliferative, anti-inflammatory, and anti-allergic properties [31]. A recent study indicated that osthole

suppressed TGF-β1-induced EMT in lung cancer A549 cells [32]. Because TGF-β1 activates furin expression in several cell lines [33, 34], and proteolytic processing of the TGF-β1 precursor by furin is an essential step in the formation of biologically active TGF-β1 [35], osthole might suppress TGF-β1-induced autocrine effects by blocking furin-like activities.

In conclusion, we screened the inhibitory effects of 124 crude drugs listed in the Japanese pharmacopoeia on *in vitro* furin-like enzymatic activities. Of these drugs, Cnidii Monnieris Fructus, which is the dried fruit of *C. monnieri* (Japanese name Jashoshi), strongly inhibited furin-like activity. We further isolated and identified two bioactive coumarins, imperatorin and osthole, from Cnidii Monnieris Fructus.

Conflict of Interest

The authors declare no conflict of interest.

References

1. HD Chen J, Luo Y, Guo H, Jiang RD, Liu MQ, Chen Y, Shen XR, Wang X, Zheng XS, Zhao K, Chen QJ, Deng F, Liu LL, Yan B, Zhan FX, Wang YY, Xiao GF, Shi ZL (2020) A pneumonia outbreak associated with a new coronavirus of probable bat origin. Nature 579:270-273
2. Shang J, Wan Y, Luo C, Ye G, Geng Q, Auerbach A, Li F (2020) Cell entry mechanisms of SARS-CoV-2. Proc Natl Acad Sci U S A 117:11727–11734
3. Hoffmann M, Kleine-Weber H, Pöhlmann S (2020) A Multibasic Cleavage Site in the Spike Protein of SARS-CoV-2 Is Essential for Infection of Human Lung Cells. Mol Cell 78:779–784.e5
4. Bestle D, Heindl MR, Limburg H, Van Lam van T, Pilgram O, Moulton H, Stein DA, Hardes K, Eickmann M, Dolnik O, Rohde C, Klenk HD, Garten W, Steinmetzer T, Böttcher-Friebertshäuser E (2020) TMPRSS2 and furin are both essential for proteolytic activation of SARS-CoV-2 in human airway cells. Life Sci Alliance 3:e202000786
5. Cheng YW, Chao TL, Li CL, Chiu MF, Kao HC, Wang SH, Pang YH, Lin CH, Tsai YM, Lee WH, Tao MH, Ho TC, Wu PY, Jang LT, Chen PJ, Chang SY, Yeh SH (2020) Furin Inhibitors Block SARS-CoV-2 Spike Protein Cleavage to Suppress Virus Production and Cytopathic Effects. Cell Rep 33:108254
6. Wu C, Zheng M, Yang Y, Gu X, Yang K, Li M, Liu Y, Zhang Q, Zhang P, Wang Y, Wang Q, Xu Y, Zhou Y, Zhang Y, Chen L, Li H (2020) Furin: A Potential Therapeutic Target for COVID-19. iScience 23:101642

7. AbdelMassih AF, Ye J, Kamel A, Mishriky F, Ismail HA, Ragab HA, El Qadi L, Malak L, Abdu M, El-Husseiny M, Ashraf M, Hafez N, AlShehry N, El-Husseiny N, AbdelRaouf N, Shebl N, Hafez N, Youssef N, Afdal P, Hozaien R, Menshawey R, Saeed R, Fouda R (2020) A multicenter consensus: A role of furin in the endothelial tropism in obese patients with COVID-19 infection. Obes Med 19:100281
8. Adu-Agyeiwaah Y, Grant MB, Obukhov AG (2020) The Potential Role of Osteopontin and Furin in Worsening Disease Outcomes in COVID-19 Patients with Pre-Existing Diabetes. Cells 9:2528
9. Hatsuzawa K, Nagahama M, Takahashi S, Takada K, Murakami K, Nakayama K (1992) Purification and characterization of furin, a Kex2-like processing endoprotease, produced in Chinese hamster ovary cells. J Biol Chem 267:16094-9
10. Takahashi S, Nakagawa T, Kasai K, Banno T, Duguay SJ, Van de Ven WJ, Murakami K, Nakayama K (1995) A second mutant allele of furin in the processing-incompetent cell line, LoVo. Evidence for involvement of the homo B domain in autocatalytic activation J Biol Chem 270:26565-9
11. Molloy SS, Bresnahan PA, Leppla SH, Klimpel KR, Thomas G (1992) Human furin is a calcium-dependent serine endoprotease that recognizes the sequence Arg-X-X-Arg and efficiently cleaves anthrax toxin protective antigen. J Biol Chem 267:16396-402
12. Garten W (2018) Characterization of proprotein convertases and their involvement in virus propagation. Activation of Viruses by Host Proteases. Springer International Publishing pp205-48

13. Cameron A, Appel J, Houghten RA, Lindberg I (2000) Polyarginines are potent furin inhibitors. J Biol Chem. 275:36741-9
14. Zhou M, Zhang Y, Wei H, He J, Wang D, Chen B, Zeng J, Gong A, Xu M (2018) Furin inhibitor D6R suppresses epithelial-mesenchymal transition in SW1990 and PaTu8988 cells via the Hippo-YAP signaling pathway. Oncol Lett 15:3192-3196
15. Pang YJ, Tan XJ, Li DM, Zheng ZH, Lei RX, Peng XM (2013) Therapeutic potential of furin inhibitors for the chronic infection of hepatitis B virus. Liver Int. 33:1230-8
16. Zhong M, Munzer JS, Basak A, Benjannet S, Mowla SJ, Decroly E, Chrétien M, Seidah NG (1999) The prosegments of furin and PC7 as potent inhibitors of proprotein convertases. In vitro and ex vivo assessment of their efficacy and selectivity. J Biol Chem 274:33913-20
17. Jean F, Stella K, Thomas L, Liu G, Xiang Y, Reason AJ, Thomas G. (1998) alpha1-Antitrypsin Portland, a bioengineered serpin highly selective for furin: application as an antipathogenic agent. Proc Natl Acad Sci U S A 95:7293-8
18. Couture F, Kwiatkowska A, Dory YL, Day R. (2015) Therapeutic uses of furin and its inhibitors: a patent review. Expert Opin Ther Pat 25:379-96
19. Bourne GL, Grainger DJ. (2011) Development and characterisation of an assay for furin activity. J Immunol Methods 364:101-8
20. Loveday EK, Diederich S, Pasick J, Jean F (2015) Human microRNA-24 modulates highly pathogenic avian-origin H5N1 influenza A virus infection in A549 cells by targeting secretory pathway furin. J Gen Virol 96:30-39
21. El Najjar F, Lampe L, Baker ML, Wang LF, Dutch RE (2015) Analysis of

cathepsin and furin proteolytic enzymes involved in viral fusion protein activation in cells of the bat reservoir host. PLoS One 10:e0115736

22. Leitlein J, Aulwurm S, Waltereit R, Naumann U, Wagenknecht B, Garten W, Weller M, Platten M. (2001) Processing of immunosuppressive pro-TGF-beta 1,2 by human glioblastoma cells involves cytoplasmic and secreted furin-like proteases. J Immunol 166:7238-43
23. Tellier E, Nègre-Salvayre A, Bocquet B, Itohara S, Hannun YA, Salvayre R, Augé N. (2007) Role for furin in tumor necrosis factor alpha-induced activation of the matrix metalloproteinase/sphingolipid mitogenic pathway. Mol Cell Biol 27:2997-3007
24. Sawada Y, Inoue M, Kanda T, Sakamaki T, Tanaka S, Minamino N, Nagai R, Takeuchi T. (1997) Co-elevation of brain natriuretic peptide and proprotein-processing endoprotease furin after myocardial infarction in rats. FEBS Lett 400:177-82
25. The Ministry of Health, Labour and Welfare (2016) The Japanese pharmacopoeia. 17th edn (English version). The Ministry of Health, Labour and Welfare, Tokyo
26. Ritz C, Baty F, Streibig JC, Gerhard D. (2015) Dose-Response Analysis Using R. PLoS One. 10:e0146021
27. Baba K, Kawanishi H, Taniguchi M, Kozawa M. (1992) Chromones from Cnidium Monnieri. Phytochem 31:1367–1370
28. Liu R, Feng L, Sun A, Kong L. (2004) Preparative Isolation and Purification of Coumarins from *Cnidium Monnieri* (L.) Cusson by High-Speed Counter-Current Chromatography. J. Chromatogr. 1055:71–76.

29. Örd M, Faustova I, Loog M. (2020) The sequence at Spike S1/S2 site enables cleavage by furin and phospho-regulation in SARS-CoV2 but not in SARS-CoV1 or MERS-CoV. Sci Rep. 10:16944.
30. Buchrieser J, Dufloo J, Hubert M, Monel B, Planas D, Rajah MM, Planchais C, Porrot F, Guivel-Benhassine F, Van der Werf S, Casartelli N, Mouquet H, Bruel T, Schwartz O. (2020) Syncytia formation by SARS-CoV-2-infected cells. EMBO J. 39:e106267
31. Sun Y, Yang AWH, Lenon GB. (2020) Phytochemistry, Ethnopharmacology, Pharmacokinetics and Toxicology of Cnidium monnieri (L.) Cusson. Int J Mol Sci. 21:1006
32. Feng H, Lu JJ, Wang Y, Pei L, Chen X. (2017) Osthole inhibited TGF β-induced epithelial-mesenchymal transition (EMT) by suppressing NF-κB mediated Snail activation in lung cancer A549 cells. Cell Adh Migr. 11:464-475
33. O'Sullivan MJ, Mitchel JA, Mwase C, McGill M, Kanki P, Park JA. (2020) In well-differentiated primary human bronchial epithelial cells, TGF-β1 and TGF-β2 induce expression of furin. Am J Physiol Lung Cell Mol Physiol. (in press)
34. Stawowy P, Margeta C, Kallisch H, Seidah NG, Chrétien M, Fleck E, Graf K. (2004) Regulation of matrix metalloproteinase MT1-MMP/MMP-2 in cardiac fibroblasts by TGF-beta1 involves furin-convertase. Cardiovasc Res. 63:87-97
35. Dubois CM, Blanchette F, Laprise MH, Leduc R, Grondin F, Seidah NG. (2001) Evidence that furin is an authentic transforming growth factor-beta1-converting enzyme. Am J Pathol 158:305-16

Tables

Table 1. Screening results of the inhibitory effects of 124 crude drugs on furin-like activity. Ethanol extracts of crude drugs (20 μg/mL) were pre-incubated with cell lysates and added to fluorogenic substrates (pyr-RTKR-MCA). Data are presented as mean ± standard deviation of at least three independent experiments.

Latin Name	Furin-like activity (%)
ACHYRANTHIS RADIX	95.2 ± 1.8
ACONITI RADIX PROCESSA	72.5 ± 3.6
AKEBIAE CAULIS	92.8 ± 1.8
ALISMATIS TUBER	101.9 ± 0.7
ALOE	83.1 ± 7.9
ALPINIAE OFFICINARI RHIZOMA	92.2 ± 1.5
AMOMI SEMEN	92.6 ± 2.5
ANEMARRHENAE RHIZOMA	95.4 ± 3.4
ANGELICAE ACUTILOBAE RADIX	101.8 ± 2.3
ANGELICAE DAHURICAE RADIX	99.8 ± 3.1
ARALIAE CORDATAE RHIZOMA	60.7 ± 4.2
ARCTII FRUCTUS	97.2 ± 4.1
ARECAE SEMEN	99.2 ± 2.3
ARMENIACAE SEMEN	93.0 ± 9.7
ARTEMISIAE CAPILLARIS FLOS	80.0 ± 8.3
ARTEMISIAE FOLIUM	79.0 ± 3.8

ASIASARI RADIX	78.8 ± 2.7
ASPARAGI RADIX	94.2 ± 1.1
ASTRAGALI RADIX	92.4 ± 4.6
ATRACTYLODIS LANCEAE RHIZOMA	94.4 ± 3.1
ATRACTYLODIS RHIZOMA	84.6 ± 3.1
AURANTII FRUCTUS IMMATURUS	86.3 ± 2.8
AURANTII PERICARPIUM	100.3 ± 3.8
BENINCASAE SEMEN	84.7 ± 0.3
BUPLEURI RADIX	95.0 ± 2.0
CANNABIS FRUCTUS	89.2 ± 1.7
CARTHAMI FLOS	93.7 ± 5.3
CASSIAE SEMEN	83.6 ± 4.9
CATALPAE FRUCTUS	84.8 ± 2.8
CHRYSANTHEMI FLOS	85.3 ± 4.9
CIMICIFUGAE RHIZOMA	96.4 ± 2.6
CINNAMOMI CORTEX	86.9 ± 5.7
CITRI UNSHIU PERICARPIUM	80.8 ± 2.7
CLEMATIDIS RADIX	85.9 ± 5.6
CNIDII MONNIERIS FRUCTUS	6.2 ± 0.3
CNIDII RHIZOMA	103.0 ± 3.3
COICIS SEMEN	93.0 ± 2.3
COPTIDIS RHIZOMA	82.9 ± 7.5
CORNI FRUCTUS	89.8 ± 1.8

CORYDALYS TUBER	86.5 ± 4.4
CRATAEGI FRUCTUS	98.1 ± 2.4
CURCUMAE RHIZOMA	78.2 ± 1.5
CYPERI RHIZOMA	90.0 ± 0.9
DIGENEA	101.1 ± 3.6
DIOSCOREAE RHIZOMA	92.1 ± 3.0
EPHEDRAE HERBA	86.8 ± 4.7
EPIMEDII HERBA	73.4 ± 11.3
ERIOBOTRYAE FOLIUM	79.7 ± 3.1
EUODIAE FRUCTUS	83.1 ± 2.5
FOENICULI FRUCTUS	79.9 ± 11.7
FORSYTHIAE FRUCTUS	42.9 ± 2.3
FRITILLARIAE BULBUS	90.3 ± 3.0
GARDENIAE FRUCTUS	89.0 ± 4.2
GASTRODIA TUBER	98.9 ± 2.7
GENTIANAE RADIX	101.1 ± 8.1
GENTIANAE SCABRAE RADIX	99.6 ± 3.3
GERANII HERBA	91.2 ± 12.4
GINSENG RADIX	99.5 ± 4.4
GINSENG RADIX RUBRA	97.0 ± 1.4
GLYCYRRHIZAE RADIX	91.3 ± 4.7
GLYCYRRHIZAE RADIX PRAEPARATA	89.3 ± 1.4
HOUTTUYNIAE HERBA	92.9 ± 11.7

HYDRANGEAE DULCIS FOLIUM	56.5 ± 1.8
KOI	95.4 ± 5.3
LEONURI HERBA	67.7 ± 6.1
LILII BULBUS	99.2 ± 2.6
LINDERAE RADIX	67.3 ± 1.3
LITHOSPERMI RADIX	92.2 ± 4.4
LONICERAE FOLIUM CUM CAULIS	94.6 ± 2.2
LYCII FRUCTUS	96.5 ± 4.8
MAGNOLIAE CORTEX	95.8 ± 4.9
MAGNOLIAE FLOS	99.7 ± 0.5
MALLOTI CORTEX	84.2 ± 8.0
MENTHAE HERBA	91.1 ± 1.9
MOUTAN CORTEX	100.4 ± 2.2
MYRISTICAE SEMEN	97.8 ± 0.5
NOTOPTERYGII RHIZOMA	95.3 ± 10.3
OPHIOPOGONIS RADIX	98.3 ± 1.7
PAEONIAE RADIX	95.3 ± 1.6
PANACIS JAPONICI RHIZOMA	85.8 ± 2.8
PERILLAE HERBA	90.1 ± 1.5
PERSICAE SEMEN	95.3 ± 2.7
PEUCEDANI RADIX	103.2 ± 5.8
PHARBITIDIS SEMEN	79.9 ± 11.2
PHELLODENDRI CORTEX	82.1 ± 6.0

PICRASMAE LIGNUM	99.4 ± 3.0
PINELLIAE TUBER	60.7 ± 3.4
PLANTAGINIS SEMEN	98.2 ± 3.6
PLATYCODI RADIX	88.7 ± 1.4
POGOSTEMONI HERBA	83.9 ± 1.2
POLYGALAE RADIX	92.7 ± 3.3
POLYGONATI RHIZOMA	87.6 ± 9.7
POLYGONI MULTIFLORI RADIX	92.1 ± 6.7
POLYPORUS	100.6 ± 1.7
PORIA	93.3 ± 2.8
PRUNELLAE SPICA	93.9 ± 4.0
PRUNI CORTEX	92.2 ± 13.0
PUERARIAE RADIX	92.2 ± 6.4
QUERCUS CORTEX	97.0 ± 1.7
REHMANNIAE RADIX	94.5 ± 1.0
RHEI RHIZOMA	88.1 ± 2.6
RYCII CORTEX	97.6 ± 4.1
SAPOSHNIKOVIAE RADIX	91.9 ± 3.5
SAUSSUREAE RADIX	79.2 ± 2.7
SCHISANDRAE FRUCTUS	90.4 ± 1.6
SCHIZONEPETAE SPICA	85.2 ± 6.6
SCUTELLARIAE RADIX	87.1 ± 8.0
SENNAE FOLIUM	80.0 ± 2.4

SESAMI SEMEN	95.7 ± 0.4
SINOMENI CAULIS ET RHIZOMA	93.1 ± 4.4
SMILACIS RHIZOMA	90.5 ± 1.7
SOPHORAE RADIX	99.1 ± 3.9
SWERTIAE HERBA	90.8 ± 4.6
TRIBULI FRUCTUS	95.1 ± 1.8
TRICHOSANTHIS RADIX	87.7 ± 9.2
UNCARIAE UNCIS CUM RAMULUS	104.1 ± 5.8
UVAE URSI FOLIUM	89 ± 6.5
VALERIANAE FAURIEI RADIX	90.7 ± 6.2
ZANTHOXYLI PIPERITI PERICARPIUM	82.4 ± 3.9
ZEDOARIAE RHIZOMA	77.1 ± 3.7
ZINGIBERIS RHIZOMA	96.8 ± 0.5
ZINGIBERIS RHIZOMA PROCESSUM	79.4 ± 6.1
ZIZYPHI FRUCTUS	97.7 ± 3.9
ZIZYPHI SEMEN	99.7 ± 1.7

1

2

Table 2 IC_{50} of different crud drugs

Sample	IC_{50} (μg/mL)
Cnidii Monnieris Fructus	1.10
Cnidii Rhizoma	>50
Hydrangeae Dulcis Folium	7.12
Forsythiae Fructus	6.52

Figure legend

Fig. 1 Structure and IC_{50} of imperatorin (1) and osthole (2)

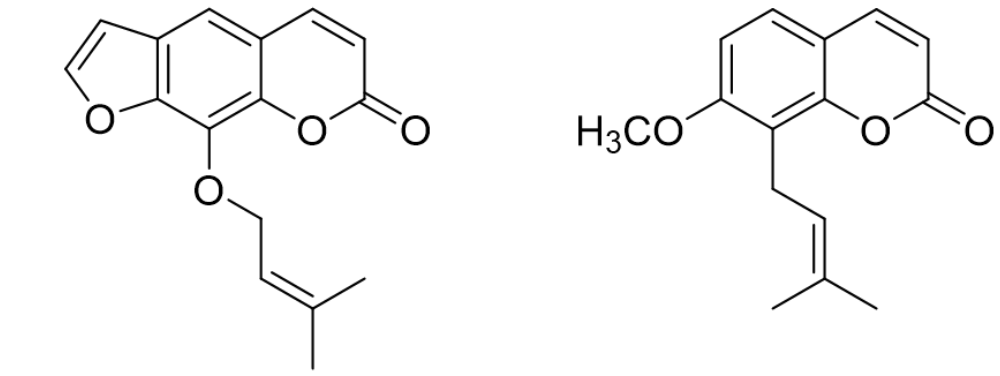

(IC_{50} = 1.45 mM) (IC_{50} = 9.45 μM)

1 **2**